Glucose Transport and Utilization in the Human Brain: Model Using Carbon-11 Methylglucose and Positron Emission Tomography

Ludwig E. Feinendegen, Hans Herzog, Helmut Wieler, Dennis D. Patton, and August Schmid

Institute of Medicine, Nuclear Research Center; and Department of Nuclear Medicine, University of Düsseldorf, Jülich, FRG; and Division of Nuclear Medicine, University of Arizona Medical Center, Tucson, Arizona

3-0-[^{11}C]-Methyl-D-glucose (CMG) is specifically suited for measuring carrier facilitated glucose (G) transport; it enters the free G pool in tissue from where it is not utilized for metabolism in contrast to G, but is transported back into circulation. The ratio of carrier affinity for G and CMG was reported to be 1.11. By simultaneously measuring CMG concentration in plasma and in cerebral cortex in vivo with positron tomography at 1-min intervals for 40 min, two time-activity curves are obtained, as reported previously, which together with the G concentration in plasma yield the in vivo rate constants of G transport across the blood-brain barrier and the rate of G inflow; a repeat measurement at a different G concentration in plasma gives the in vivo Michaelis-Menten constant K_M and the maximal rate of transport V_{MAX}. The present paper summarizes and extends this approach to analyzing the free G pool in tissue, the rate of G return to circulation, and the rate of G exit into metabolism with its corresponding rate constants. The data from six volunteers agreed with results reported for the individual biochemical parameters in primate brains.

J Nucl Med 27:1867–1877, 1986

The in vivo measurement of the metabolic rate of glucose (G) utilization in brain tissue has been greatly advanced by labeled 2-deoxyglucose, and especially by [^{18}F]-2-deoxy-2-fluoro-D-glucose (FDG) used with positron emission tomography (PET) (*1–3*). The study of G metabolism in brain is complicated by the interaction between transport and utilization. In order to study G transport from blood to brain and back again, a tracer is needed that is transported by the same facilitated-transport mechanism as G, but not metabolized. The tracer 3-0-[^{11}C]-methyl-D-glucose (CMG) is well suited to studies of G transport (*4–9*). Its transport into brain tissue is very similar to that of G; however, in brain it is not metabolized but is transported back into the circulation by the same carrier (*5*). Unlike FDG, which is phosphorylated by hexokinase, CMG has been shown in animal experiments to label the free G pool, after establishment of an equilibrium distribution between plasma and tissue (*10*).

This article develops the CMG transport model further and applies it to PET measurement of the free steady-state G pool in brain tissue, and the rate of net G transfer from this pool into the metabolic pathway. Following an intravenous pulse injection of CMG, its concentration in tissue, C_T*, rises relative to its concentration in plasma, C_P*. (Variables with an asterisk relate to CMG, those without to glucose. See Appendix A for list of variables). In fact, the rate of increase of C_T* against C_P* has been shown to be determined by [k_2*], the rate constant governing the outflow of CMG from tissue back into the circulation (*7–9*). When dynamic equilibrium is reached, the ratio between C_P* and C_T* becomes constant and C_T* is then designated by C_{TE}*. Since G and CMG share the same carrier for facilitated transport, the three parameters C_P*, C_{TE}*, and [k_2*], together with the G concentration in plasma, C_P, permit calculation of the facilitated transport of G into tissue,

Received Jan. 31, 1985; revision accepted May 22, 1986.

For reprints contact: L. E. Feinendegen, MD, Institute of Medicine, Nuclear Research Center, Jülich GmbH, D-5170 Jülich, FRG.

V_I, and the apparent rate constant of inflow, κ_1. Moreover, two measurements taken at different plasma G levels yield the half-saturation amount of substrate, i.e., the Michaelis-Menten constant K_M and the related maximal velocity of transport V_{MAX}.

MATERIALS AND METHODS

The model is shown in Fig. 1, which also gives the principal measurements schematically; an example of experimentally measured data is given in Fig. 2.

Glucose Transport into Tissue

The model assumes facilitated transport of G and CMG from the capillary plasma into the tissue by the same carrier (*11–15*), and the establishment of an equilibrium distribution of CMG between C_P^* and C_T^*, the latter becoming C_{TE}^* (*5,7–10*). Following an intravenous pulse injection of CMG, the slope of C_T^* versus time rises to C_{TE}^* (Fig. 2). Since G and CMG share the same carrier, with similar inflow kinetics, and since the concentration of G does not saturate the binding sites of the carrier, the inflow kinetics of both G and CMG are of first order (velocity depends on carrier availability and on substrate concentration). With conventional Michaelis-Menten equations for first-order reactions catalyzed by enzymes, this slope yields the rate constant that governs CMG transport from tissue back into blood (*7–9*). This constant, as shown in Appendix B, contains the term for the concentration of free carrier,

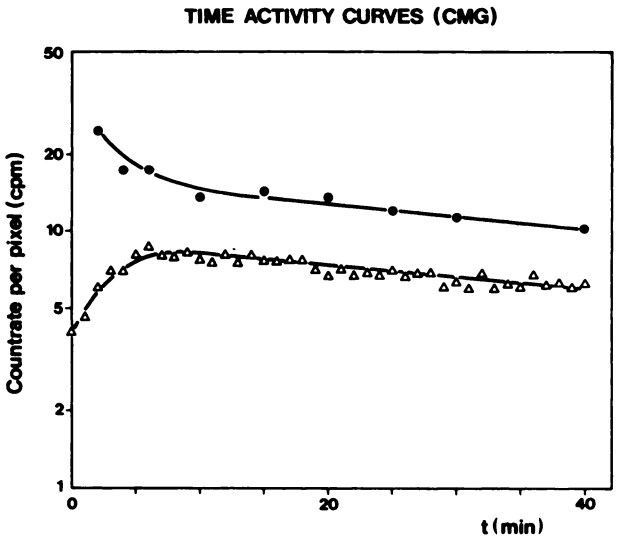

FIGURE 2
Time-activity curves obtained from cerebral cortex, C_T^* (Δ), and from plasma arterialized venous, calibrated to ECAT) CMG concentration, C_p^* (●), as function of time; corrected for isotopic decay. Initial rise of C_T^* to state of equilibrium distribution of tracer between blood and tissue, C_{TE}^*, is used for calculation of $[k_2]$ as schematically presented in Appendix B

Hcf, in the two-directional mode of transport in the tissue examined (*16*); Hcf is assumed to be the same for tracer inflow, v_I, and outflow, v_E (*5*). The measured rate constant is here termed $[k_2^*]$. It is to be understood

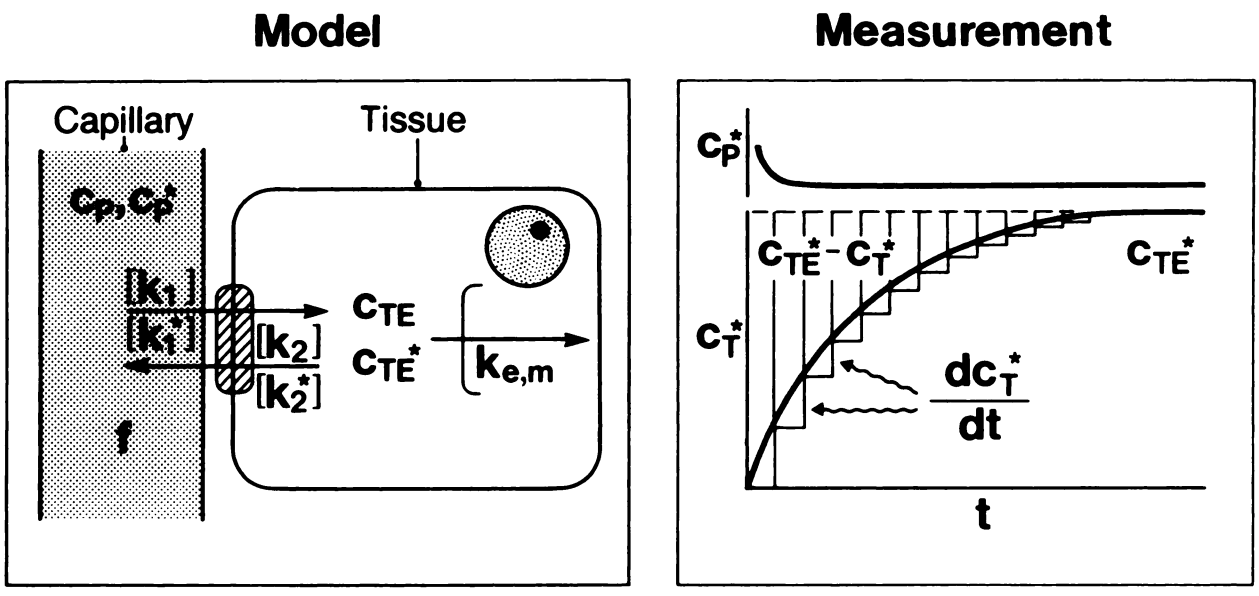

FIGURE 1
Model and approach to calculating $[k_2]$; see Appendix B. C_p (C_p^*) = G (CMG) concentration in plasma; μmol/mol (cpm/ml). C_{TE} (C_{TE}^*) = G (CMG) concentration in tissue at equilibrium distribution between tissue and blood; CMG concentration in tissue, C_T^*, rises to C_{TE}^* following pulse injection; μmol/g (cpm/g). k_1, $[k_1^*]$ and k_2, $[k_2^*]$ = rate constants governing facilitated transport of G (CMG) into, and out of, tissue; min^{-1}. $k_{E,M}$ = rate constant governing the net transfer of G into metabolism by hexokinase; min^{-1}. f = regional blood flow; ml/g/min. t = time of measurement; min. C_p (C_p^*)·f·τ, with units μmol/g (cpm/g), is equal to substrate available for transport per minute, with τ = time unit (minute)

that according to Michaelis-Menten kinetics this $[k_2^*]$ is essentially given by $\frac{V_{MAX}}{K_M + S}$, with S here being the available substrate concentration at either side of the blood-brain barrier, in the case of the reversible, or two-directional, enzyme-catalyzed transport (*16*). The same argument applies to the rate constant that governs CMG inflow, which is here termed $[k_1^*]$ (see Appendix B).

It is understood that in the general form of the rate equation, the rate constant that characterizes the activity of the carrier system for G influx, $[k_1]$, is described by the following expression (*16*):

$$[k_1] = \frac{V_{MAX1}}{K_{M1}\left(1 + \frac{S_1}{K_{M1}} + \frac{S_2}{K_{M2}}\right)}. \quad (1)$$

V_{MAX1}, K_{M1}, and S_1 relate to the inflow side of the barrier and K_{M2} and S_2 to the outflow side.

The rate constant for the outflow side is then given by

$$[k_2] = \frac{V_{MAX2}}{K_{M2}\left(1 + \frac{S_1}{K_{M1}} + \frac{S_2}{K_{M2}}\right)}. \quad (2)$$

Yet, according to experiments which were carried out in rat brains (*5*), the kinetic constants K_{M1}, V_{MAX1}, and K_{M2}, V_{MAX2} for G inflow and outflow are the same; i.e., $K_{M1} = K_{M2} = K_M$ and $V_{MAX1} = V_{MAX2} = V_{MAX}$. Moreover, when assessing unidirectional facilitated G transport the G concentration on the opposite side of the barrier was proposed to be of negligible consequence (*1*) so that it appears to be valid to state

$$[k_2] = \frac{V_{MAX}}{K_M + C_{TE}}. \quad (3)$$

The two rate constants $[k_1^*]$ and $[k_2^*]$ are proportional to the product of capillary surface area and permeability. The product of either of these rate constants and ζ, the ratio of carrier affinity for G to that of CMG, which was reported from rat experiments to be 1.11 (*5,8,9*), provides the corresponding rate constant for G, $[k_2]$ or $[k_1]$. A similar value was reported also by others (*17*).

Appendix B summarizes the derivation of $[k_2]$ and the kinetic parameters for G transport (*7–9*). The data will be used for extending the model to the analysis of C_{TE}, $v_{E.M}$ and $k_{E.M}$; the equations for this are summarized in Appendix C and more fully explained below. Convenient but not necessary for the derivation is the determination of K_M and V_{MAX} for the carrier (*8,9*), as will be shown below. The quantities $v_{E.M}$ and $k_{E.M}$ describe the net G transfer into metabolism, a reaction that is governed by the enzyme hexokinase (*1*).

Free G Pool in Tissue and G Transfer into Metabolic Pathway

The value of C_{TE}, the steady-state glucose concentration in tissue, determines $[k_2]$. C_{TE} is not measured directly but is given by the product of C_P with the distribution volume of G in tissue, VD_G, i.e.,

$$C_{TE} = C_P \cdot VD_G. \quad (4)$$

At steady state the rate of G inflow into tissue, v_I, equals the sum of rate of outflow back into circulation, v_E, and of transfer to metabolic pathways, $v_{E.M}$, i.e.,

$$v_I = v_E + v_{E.M}. \quad (5)$$

Since both v_E and $v_{E.M}$ depend on C_{TE}, and taking v_I from Eq. B:20 (Notation: Eq. B:11 refers to Appendix B, Equation 11), the above equation becomes

$$[k_2] \cdot C_P \cdot \frac{C_{TE}^*}{C_P^*} = [k_2] \cdot C_{TE} + k_{E.M} \cdot C_{TE} \quad (6)$$

(see Eq. C:2). Dividing both sides of the equation by $[k_2]$ gives

$$C_P \cdot \frac{C_{TE}^*}{C_P^*} = C_{TE} + \frac{k_{E.M}}{[k_2]} \cdot C_{TE} \quad (7)$$

or

$$C_P \cdot \frac{C_{TE}^*}{C_P^*} = C_{TE} \cdot \left(1 + \frac{k_{E.M}}{[k_2]}\right) \quad (8)$$

(see Eq. C:3); and

$$C_{TE} = C_P \cdot \frac{C_{TE}^*}{C_P^*} \cdot \frac{1}{1 + \frac{k_{E.M}}{[k_2]}} \quad \text{(see Eq. C:4).} \quad (9)$$

This is the first of two equations permitting the estimation of C_{TE}. Moreover, rearranging this equation gives the distribution volume for G in tissue,

$$VD_G = \frac{C_{TE}}{C_P} = \frac{C_{TE}^*}{C_P^*} \cdot \frac{1}{1 + \frac{k_{E.M}}{[k_2]}}. \quad (10)$$

The above equations contain two unknowns, namely C_{TE} and $k_{E.M}$, and cannot be solved directly. The difficulty may be overcome by approximation of the quotient $\frac{k_{E.M}}{[k_2]}$ and thus of the expression $\frac{1}{1 + \frac{k_{E.M}}{[k_2]}}$. For a given $[k_2]$, $k_{E.M}$ may have different values; but both are expected to respond in the same direction with changing values of C_{TE} so that the quotient remains relatively constant, even though the individual values of $[k_2]$ and $k_{E.M}$ may vary.

The maximum value of $k_{E.M}$ is $1 - [k_2]$ for the special case in which the amount of G transported per unit mass of tissue is equal to C_{TE}. However, this is excluded in principle, for it would mean instantaneous utilization of G as it enters the free G pool in tissue and would exclude any G reserve in tissue.

Table 1 lists ranges of theoretically possible $k_{E.M}$ values for different values of $[k_2]$. Assuming here that

TABLE 1
Values of F for Different Values of $[k_2]$ and $k_{E,M}$

$$F = \frac{1}{1 + \frac{k_{E,M}}{[k2]}}.$$

$[k_2]$	$k_{E,M}$	F	F_{mean}
	0.10	0.50	
	0.20	0.33	
	0.30	0.25	
0.10	0.40	0.20	0.25 ± 0.13
	0.50	0.17	
	0.60	0.14	
	0.70	0.13	
	0.10	0.67	
	0.20	0.50	
	0.30	0.40	
0.20	0.40	0.33	0.41 ± 0.16
	0.50	0.29	
	0.60	0.25	
	0.10	0.75	
	0.20	0.60	
0.30	0.30	0.50	0.53 ± 0.15
	0.40	0.43	
	0.50	0.38	
	0.10	0.80	
	0.20	0.67	
0.40	0.30	0.57	0.64 ± 0.13
	0.40	0.50	
	0.10	0.83	
0.50	0.20	0.71	0.72 ± 0.10
	0.30	0.63	
	0.10	0.86	
0.60	0.20	0.75	0.81 ± 0.08

* See text, Eqs. (10) and (11).

all possible values have equal probability, the ratio of $\frac{k_{E,M}}{[k_2]}$ and thus the expression $\frac{1}{1 + \frac{k_{E,M}}{[k_2]}}$, which will be called F, is averaged for the different $[k_2]$ values and is given as factor F ± standard deviation or range values, to be inserted into the corresponding equation (Eq. C:5). Various reports, however, indicate similarity between the values of $[k_2]$ and those of $k_{E,M}$ (*18,19*). The table shows that with increasing $[k_2]$ the mean value of F increases, and its error range diminishes, from 0.25 ± 0.13 for $[k_2] = 0.1$ to 0.81 ± 0.08 for $[k_2] = 0.6$. With these $[k_2]$-specific mean values of F, the values of C_{TE} can be calculated for different values of $[k_2]$. Hence

$$C_{TE} = C_P \cdot \frac{C_{TE}^*}{C_P^*} \cdot F \quad \text{(see Eq. C:5).} \qquad (11)$$

The second approach to C_{TE} uses the average values of V_{MAX} and K_M of the transport system from blood to tissue as they were determined in a number of normal individuals, each studied at two different blood G levels (see Eqs. B:25–33).

V_{MAX} and K_M of the transport system can be calculated principally from measurements of the relationship between v_I and S available for transport into tissue.

The general expression for v_I is

$$v_I = \frac{V_{MAX} \cdot S}{K_M + S} \quad \text{(see Eq. B:25).} \qquad (12)$$

In order to define S, and since $v_I = [k_1] \cdot S$, then according to Eq. B:17,

$$v_I = [k_1] \cdot f \cdot \tau \cdot C_P \qquad (13)$$

where f is flow; or

$$S = f \cdot \tau \cdot C_P. \qquad (14)$$

C_P is directly available; the expression $f \cdot \tau$ is obtained from rearranging the CMG equilibrium equation, as given in Eq. B:9; thus

$$f \cdot \tau = \frac{[k_2^*]}{[k_1^*]} \cdot \frac{C_{TE}^*}{C_P^*}. \qquad (15)$$

Therefore

$$S = \frac{[k_2^*]}{[k_1^*]} \cdot \frac{C_{TE}^*}{C_P^*} \cdot C_P \quad \text{(see Eqs. B:28–30).} \qquad (16)$$

This equation, however, contains the unknown ratio $\frac{[k_2^*]}{[k_1^*]}$.

It is noted that κ_1 is different from $[k_1]$ (see Appendix A), but if the ratio $\frac{[k_2^*]}{[k_1^*]}$ is assumed to be close to 1, at least in normal individuals (*7–9*), then S is approximately $\frac{C_{TE}^*}{C_P^*} \cdot C_P$. The value of K_M calculated under this assumption will be called K_M', as shown below. (This assumption will be challenged in Discussion.)

Equation (12) can be inverted (Lineweaver-Burk transformation), to yield $\frac{1}{v_I}$ as a linear function of $\frac{1}{S}$:

$$\frac{1}{v_I} = \frac{1}{V_{MAX}} + \frac{1}{S} \cdot \frac{K_M'}{V_{MAX}}. \qquad (17)$$

The resulting slope in the Lineweaver-Burk plot is $\frac{K_M'}{V_{MAX}}$, whereas the intercept is $\frac{1}{V_{MAX}}$ (see Eq. B:33).

Accepting that V_{MAX} and K_M' for the hexose transport is the same for both sides of the barrier, as was discussed above (*5*), and since $v_E = C_{TE} \cdot [k_2]$,

$$v_E = \frac{V_{MAX} \cdot C_{TE}}{K_M' + C_{TE}} \qquad (18)$$

and

$$[k_2] = \frac{V_{MAX}}{K_M' + C_{TE}} \quad \text{(see Eq. C:7)} \qquad (19)$$

or

$$C_{TE} = \frac{V_{MAX}}{[k_2]} - K_M' \quad \text{(see Eq. C:8).} \qquad (20)$$

This is the second equation permitting the assessment of C_{TE}.

Then $v_{E,M}$ and $k_{E,M}$ are calculated as follows:

$$v_{E,M} = v_I - v_E. \qquad (21)$$

By substituting v_I and v_E (see Eqs. B:20 and C:9–12),

$$v_{E,M} = [k_2] \cdot \frac{C_{TE}^*}{C_P^*} \cdot C_P \cdot (1 - F). \qquad (22)$$

Then $k_{E,M}$ can be determined since

$$k_{E,M} = \frac{v_{E,M}}{C_{TE}} \quad \text{(see Eq. C:13).} \qquad (23)$$

Measurements

The technique of sequential scintigraphy by PET (ECAT II, Ortec) has been described (*7–9*). Briefly, CMG was synthesized by methylation through [C-11]-CH_3 of the potassium salt of 1,2:5,6,-diiso-propylidene-D-glucose (*6*). Between 6 and 14 mCi (220 and 520 MBq) CMG were prepared in sterile saline solution after chromatographic purification and sterile filtration. Not less than 5 mCi (185 MBq) were injected into an antecubital vein. The examination was carried out under the following conditions: ambient light, laboratory noise, patient's eyes open, ears unplugged. The model was validated in six normal volunteers (three male, three female, age range 21–44 yr). Informed consent was obtained in all cases, and each subject was studied twice, at two different levels of blood glucose.

The transaxial activity distribution in one selected slice parallel to the canthomeatal line was monitored by PET (medium-resolution shadow shields, high-resolution data collection, measured attenuation coefficient for image reconstruction) at the rate of 1 image per min over 40 min, yielding the rise of C_T^* against C_P^*, when corrected for the decay of ^{11}C, as shown in Fig. 2. The initial rapid increase of C_T^* was followed by a slow rate of decrease that is accompanied by the same rate of decrease of C_P^*.

C_P^* was recorded for 40 min at increasing intervals (1–5 min) from the venous blood of a hyperemic hand (*3*) and was also corrected for decay of the ^{11}C. Because C_P^*, like C_T^*, was initially measured at 1-min intervals beginning after 1 min, the curves of arterialized versus arterial blood could be shown and are taken here to be identical (*20*). This means that the effect of blood flow through multiple paths of varying length from the arterial to the venous side on tracer concentration in arterialized versus arterial blood can be neglected after 1 min (*20*), and also that the time delay between the peak of the arterial concentration and that of the collected arterialized blood from the warmed hand (up to a maximum of 30 sec after injection) does not affect the measurement of C_P^*.

In order to calculate $[k_2]$ (see Eqs. B:14 and B:15), one must first find a good mathematic model for the curve of C_T^* versus time. Here the C_T^* curve was approximated by three exponential functions because a biexponential C_P^* curve with rate constants b_1 and b_2 was used as input function (*8,9*). Thus, inserting C_P^* into the solution of Eq. B:8, namely

$$C_T^*(t) = \kappa_1 \int_0^t C_P^*(t') \exp\{-[k_2^*] \cdot (t - t')\}\, dt' \qquad (24)$$

gives

$$C_T^*(t) = A_1 \exp(-[k_2^*]t) + A_2 \exp(-b_1 t) + A_3 \exp(-b_2 t). \qquad (25)$$

Because of the low extraction rate of CMG it is necessary to correct for tracer in the vascular compartment at least during the first 5 min, by estimating a total blood volume of 5% or less of the tissue volume in gray and white matter (*1–3,21*).

Plasma G is measured as usual from venous blood samples at intervals of 1 to 15 min.

After the initial rise of C_T^* for ~10 min, a dynamic equilibrium of CMG distribution between tissue and blood is reached and is evident from a practically constant value of $\frac{C_{TE}^*}{C_P^*}$. From then on CMG traces the extravascular distribution space; initial heterogeneity of tracer distribution has been reported previously (*7–9*). In the present measurements, the entire cerebral cortex in the selected slice is assayed and local changes in C_{TE}^* can be scaled against the average of the entire cortex.

It is to be noted, as shown in Fig. 3, that the nonmetabolizable CMG is eliminated from the blood pool more slowly than is FDG, so that its blood concentration remains relatively high during the whole period of measurement.

For determining the K_M' and V_{MAX} for the hexose carrier from blood to tissue, sequential scintigraphy is repeated on the same patient ~2 hr later, ~7 to 10 min after i.v. injection of 10 g of glucose in a 20% solution; in order to maintain the elevated plasma G at a constant level a 5% G solution is given thereafter by continuous i.v. drip during the examination. Although this procedure cannot achieve a totally constant G level, it does lead to an acceptable average value during the period of measurement. This mean value is entered into the analysis of C_P (Fig. 4).

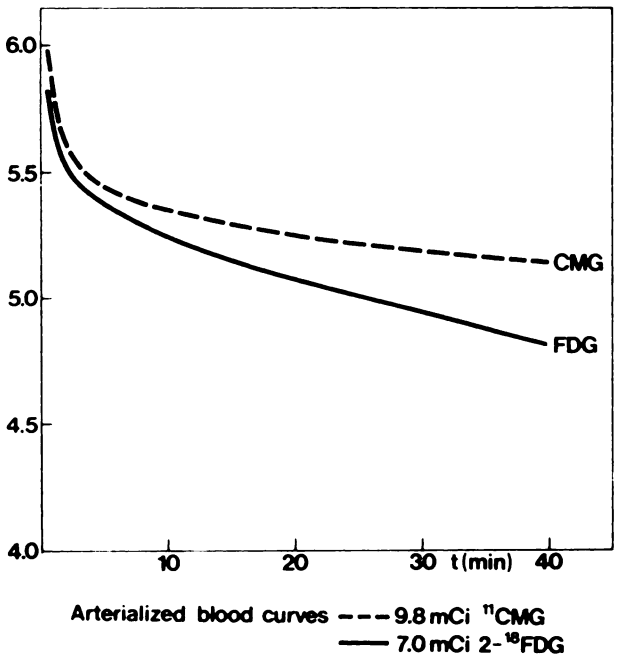

FIGURE 3
Plasma curves (hyperemic hand) of FDG (——) versus CMG (- - -) in same patient (7.0 mCi FDG versus 9.8 mCi CMG). Ordinate: plasma sample count rate in arbitrary units, normalized to same initial count rate and corrected for decay

RESULTS

Figure 5 shows a normal C_{TE}* image taken at 10–25 min; it illustrates the heterogeneity of CMG distribution. Table 2 presents the four measured data [k_2*], C_{TI}*, C_P*, and C_P and the calculated average value of [k_2], v_I, κ_I, V_{MAX}, K_M', C_{TE}, $v_{E,M}$ and $k_{E,M}$ for the entire cortical area in the brain of each of the six normal volunteers. The overall average values are also listed.

Since κ_I contains the flow term f (see Eqs. B:18 and B:24), the ratio $\frac{\kappa_I}{[k_2]}$ relates to cortical perfusion (*7–9*).

The values of C_{TE} in Table 2 were calculated according to the first approach, using the measured values of C_P, C_{TE}*, and C_P*, and the value approximation of F (see Eq. 11 and Table 1). When the second approach using V_{MAX}, K_M' and [k_2] was taken (see Eq. 20), C_{TE} was consistently larger by a factor of ~2. This discrepancy between the C_{TE} values derived using the two approaches can be traced to a systematic error rooted in the assumption in the second approach that [k_2*] is approximately equal to [k_1*]; it is also noted that [k_2*] exhibits a relatively large range of variation. The C_{TE} values given in Table 2 are taken to be the more reliable ones. The data in Table 2 are in good agreement with published results from both animal experiments and human measurements using different methods (*1–5,10,13,17,18,22*).

DISCUSSION

The present technique employs a dual-parameter analysis of CMG concentration in blood and tissue during the time period in which dynamic equilibrium of tracer distribution is reached (*23*). It is similar to the approach to measuring oxygen consumption (*22*) and obviates the need for conventional analysis of a tracer transit time through successive metabolic compartments. Moreover, the CMG technique takes advantage of the fact that in viable tissue this tracer is transported, even if slightly less efficiently, in a manner similar to that of G. In converting the [k] values for facilitated transport of CMG to G the correction factor $\zeta = 1.11$ was used (*5,8,9*). This factor is similar to that reported by others (*17*).

CMG is not metabolized in the brain but returns from the tissue pool back into circulation (*5*). Thus, the change of C_T* relative to C_P* is used for measuring [k_2*], which yields [k_2] when multiplied by ζ. The four parameters C_{TE}*, C_P*, [k_2], and C_P are needed to describe the kinetics of the entire sequence of steps of G uptake into the free G pool and its subsequent transfer

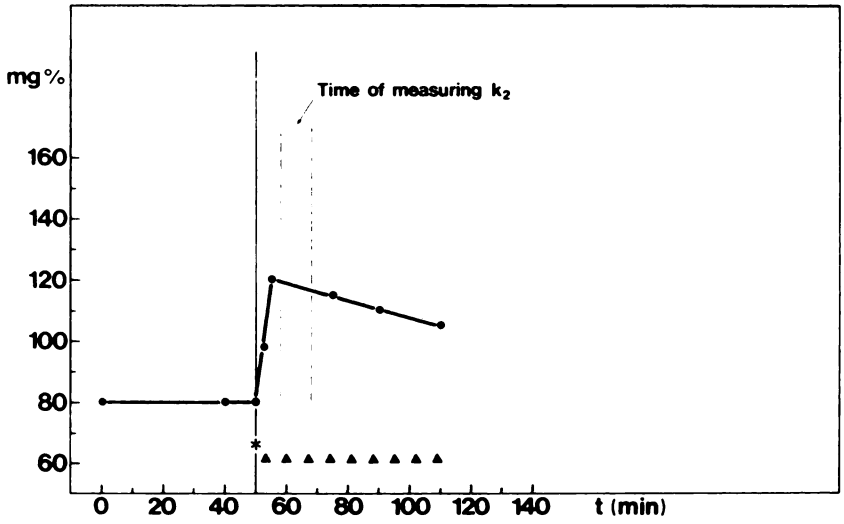

FIGURE 4
Illustration of infusion schedule used to obtain acceptably constant arterialized plasma concentration of glucose. Ordinate is plasma glucose (mg %). * = 8g glucose; ▲ = Continuous i.v. drip of 5%-solution (0.1 ml/sec)

FIGURE 5
Image of CMG distribution in orbito-meatal (OM) + 4.5 cm transaxial plane of normal brain. Anterior is at top of figure; left is to reader's left

into metabolism. The net rate of transfer of G from the free tissue G pool into metabolism, $v_{E,M}$, is given by the difference between glucose transport across the blood-brain barrier into and out of tissue, i.e., v_I minus v_E at steady state.

The values of V_{MAX} and K_M' were determined from the Lineweaver-Burk plot of $\frac{1}{v_I}$ versus $\frac{1}{S}$ (see Eq. 17). In specifying S the assumption was made that $[k_2]$ and $[k_1]$ are approximately equal. Since the ratio of $[k_2]$ to $[k_1]$ determines the slope of the regression line, but not the intercept, it affects K_M' but not V_{MAX}. The approach to C_{TE} using V_{MAX} and K_M' fails to lead to the same C_{TE} value as that derived directly from the measured values of C_P, C_{TE}*, C_P*, and a reasonably valid approximation of F. Indeed, from the data in Table 2 it appears that the derived K_M' values are consistently too low, so that the previously made assumption of equality between $[k_2]$ and $[k_1]$ should not be maintained.

There is good agreement between the present data for G transport, free G pool and G metabolism in humans and the published results that were obtained by different methods in animals and humans (*1–5,10,13,17,18,22*). This supports the validity of the approach of averaging the ratio $\frac{k_{E,M}}{[k_2]}$ for a given $[k_2]$ value, and of the value of ζ, both of which introduce uncertainties into the present work. An important achievement of this work is the confirmation of existing data by another, novel technique which, of course, suffers from similar ranges of errors and assumptions as, for example, the method using FDG. It is to be stressed that the operational equations and data here presented do not rely on values obtained elsewhere, except for the constant ζ. It is likely that $v_{E,M}$ and $k_{E,M}$ correctly describe the metabolic utilization of G from the free G pool. In all, the data are generally quite similar to those obtained by the widely-used FDG method for specifically measuring cerebral G uptake by phosphorylation in the brain of primates (*1–3,18*), even

TABLE 2
Numerical Values of Kinetic Parameters*

		Patients												$\bar{x} \pm \sigma$	
		1		2		3		4		5		6			
N = Normal C_p E = Elevated C_p		N	E	N	E	N	E	N	E	N	E	N	E	N	E
$[k_2^*]$	[min^{-1}]	0.25	0.23	0.25	0.19	0.34	0.27	0.43	0.34	0.35	0.29	0.32	0.31	0.32 ± 0.06	0.27 ± 0.05
C_{TE}^*/C_{PE}^*	[ml/g]	0.46	0.47	0.51	0.42	0.39	0.43	0.52	0.40	0.41	0.46	0.41	0.38	0.45 ± 0.06	0.43 ± 0.03
C_p	[μmol/ml]	4.0	5.0	3.6	7.2	2.7	4.7	4.2	7.7	5.0	6.6	4.7	6.1	4.03 ± 0.82	6.22 ± 1.19
$[k_2]$	[min^{-1}]	0.28	0.26	0.28	0.21	0.38	0.30	0.48	0.38	0.39	0.32	0.36	0.35	0.36 ± 0.08	0.30 ± 0.06
v_I	[μmol/min g]	0.52	0.62	0.51	0.64	0.40	0.62	1.06	1.18	0.80	0.98	0.70	0.80	0.67 ± 0.24	0.81 ± 0.23
k_1	[min^{-1}]	0.13	0.12	0.14	0.09	0.15	0.13	0.25	0.15	0.16	0.15	0.15	0.13	0.16 ± 0.04	0.13 ± 0.02
V_{MAX}	[μmol/min g]	2.22		1.05		1.40		1.64		1.86		3.59		1.96 ± 0.89	
K_M'	[μmol/g]	6.17		1.93		2.63		1.21		2.74		8.01		3.78 ± 2.68	
C_{TE}	[μmol/g]	0.97	1.26	0.98	1.23	0.66	1.09	1.61	1.94	1.30	1.62	1.24	1.22	1.13 ± 0.33	1.39 ± 0.32
$v_{E,M}$	[μmol/min g]	0.24	0.29	0.24	0.38	0.15	0.29	0.30	0.43	0.29	0.46	0.26	0.38	0.25 ± 0.05	0.37 ± 0.07
$k_{E,M}$	[min^{-1}]	0.25	0.23	0.25	0.31	0.22	0.26	0.19	0.22	0.22	0.28	0.21	0.31	0.22 ± 0.02	0.27 ± 0.04

* Obtained with CMG in six normal volunteers, each measured at two different levels of blood glucose, including input parameters $[k_2^*]$, C_{TE}^*/C_p^* at equilibrium, and C_p; calculated parameters of glucose transport across blood-brain barrier $[k_2]$, v_I, k_1, V_{MAX} and K_M'; free glucose pool in tissue, C_{TE}; and parameters of glucose transfer into metabolism, $v_{E,M}$ and $k_{E,M}$. For these calculations the value of F in Table 1 closest to the value of $[k_2]$ was used.

if it is true that dephosphorylation in brain tissue plays a considerable role in depressing the retention of FDG as was recently reported (*24*).

In this paper no attempt is made to analyze the distributional heterogeneity of C_{TE}* in the brain; it is most likely due to local variations of the transport function. Appendix B indicates that the values of $[k_2^*]$, C_P*, and f are crucial. A change in any of these values would alter C_{TE}*. The value of f is probably most important since neuronal activity is known to affect local perfusion (*25*).

The sequential steps in the passage of G from the circulation into the free G pool in tissue and from there into metabolism could not previously be assessed in one examination; the differentiation between those sequential steps may be diagnostically helpful in situations such as transient and separate changes in local blood flow, G transport and G metabolism. In the normal state, these three parameters are interdependently controlled.

The method may be applied to other tissues; for example the consequence of various forms of diabetes and the action of insulin on G transport may be studied in vivo. Also, in myocardium with reversible ischemia a reduction of v_I was seen (*26*); but an increase of the rate of utilization of FDG was reported for ischemic regions (*27*) and was perhaps due to diminution of C_{TE} with an increase in hexokinase activity. The term $\frac{\kappa_1^*}{[k_2^*]}$, as shown in Appendix B, expresses a distribution volume; if this value is given per unit time, it describes flow as has been shown in normal brain (*9*). Further work is needed for clarifying whether the ratio $\frac{\kappa_1^*}{[k_2^*]}$ also expresses flow under pathological conditions.

[^{18}F]-3-Deoxy-3-fluoro-D-glucose (3-FDG) was shown to behave kinetically in a manner similar to CMG (*8,28,29*) and thus may perhaps be used instead of CMG. With the advantage of the relatively long half-life of ^{18}F (110 min), which reduces decay loss of the tracer during transport from the site of its production, the technique described here could be performed even where the PET is relatively distant from the cyclotron.

The task of simultaneously assessing G transport, free G pool in tissue and transfer into metabolism in small tissue regions would require amounts of either one of these tracers larger than were maximally available in these studies, as well as a PET system with relatively high resolution and efficiency.

ACKNOWLEDGMENTS

The authors greatly appreciate the cooperation of Prof. G. Stöcklin and his group from the Institute of Chemistry, KFA, the efficient technical assistance of Mrs. Ch. Behrendt, Mrs. I. Janz, Mrs. A. Lamb, Dr. K.-J. Langen, Mr. J.-R. Magloire, Mr. O. Muzik, and Dr. E. Rota; the discussions with Mr. V. Becker and Dr. J. Booz from this Institute; the clinical cooperation of Prof. C. Morgenstern from the University Hospital, Düsseldorf; and the secretarial assistance of Mrs. B. Jansen.

This work was supported in part by the German Science Foundation and by an award from the Alexander von Humboldt Foundation, Bonn, Federal Republic of Germany.

APPENDIX A

Abbreviations

G = Glucose
CMG = 3-0-[^{11}C]-methyl-D-glucose
FDG = [^{18}F]-2-deoxy-2-fluoro-D-glucose
PET = positron emission tomography

In the following abbreviations, symbols with asterisk apply to CMG; symbols without asterisk apply to G.

C_P (C_P*) = G (CMG) concentration in plasma.
C_{TE} (C_{TE}*) = free G (CMG) pool in brain tissue at equilibrium.
C_T (C_T*) = G (CMG) concentration in tissue prior to equilibrium.
v_I = rate of G inflow into tissue.
v_E = rate of G outflow into circulation.
$v_{E.M}$ = rate of G transfer from C_{TE} into metabolism.
κ_1 = apparent rate constant of G inflow into tissue; it relates directly to C_P and contains the term for flow.
K_M = Michaelis-Menten constant for hexose carrier.
K_M' = K_M calculated under the assumption that $[k_2^*]$ is approximately equal to $[k_1^*]$; see text.
V_{MAX} = maximal velocity of transport, related to K_M.
$[k_1]$ ($[k_1^*]$) = rate constant governing G (CMG) inflow into tissue; it is independent of flow.
$[k_2]$ ($[k_2^*]$) = rate constant governing G (CMG) outflow into circulation.
ζ = ratio of carrier affinity for G to that of CMG.
$k_{E.M}$ = rate constant governing G transfer into metabolism.
f = blood flow; ml/min·g.
τ = time unit; min.

APPENDIX B

Derivation of Kinetic Parameters for Glucose Transport

For symbols see Appendix A, Fig. 1, and text.

Approach of C_T* to C_{TE}* at Equilibrium with C_P* (*7–9*)

The rate of inflow of glucose, v_I, conforms to an enzyme-like reaction (*4,5*). Thus, in analogy to enzyme reaction kinetics,

$$v_I = k_1 \cdot Hcf \cdot S \qquad (B:1)$$

(with Hcf = free carrier available for the reaction), in the two-directional mode of transport (*11*), S = substrate available for

transport mode; k_1 = rate constant of unidirectional transport (note difference between k_1 and $[k_1]$, below).
Let

$$[k_1] = k_1 \cdot Hcf, \tag{B:2}$$

then

$$v_I = [k_1] \cdot S. \tag{B:3}$$

S, the amount of substrate available for unidirectional transport from blood into tissue, is given by

$$S = C_P \cdot f \cdot \tau. \tag{B:4}$$

Thus the units of S are $\frac{\mu mol}{ml} \cdot \frac{ml}{min \cdot g} \cdot min = \frac{\mu mol}{g}$.

Using CMG as tracer

$$v_I^* = [k_1^*] \cdot f \cdot \tau \cdot C_P^*. \tag{B:5}$$

The term $[k_1^*] \cdot f \cdot \tau$ conforms to the apparent rate constant of tracer influx κ_1^*. The efflux function for CMG, v_E^*, in Fig. 1, is accordingly described as

$$v_E^* = [k_2^*] \cdot C_T^*. \tag{B:6}$$

Since

$$\frac{dC_T^*}{dt} = v_I^* - v_E^*, \tag{B:7}$$

therefore

$$\frac{dC_T^*}{dt} = [k_1^*] \cdot f \cdot \tau \cdot C_P^* - [k_2^*] \cdot C_T^*. \tag{B:8}$$

Equilibrium Between C_P^* and C_T^* as $C_T^* \rightarrow C_{TE}^*$ (7–9)

At equilibrium, $C_T^* = C_{TE}^*$ and $\frac{dC_T^*}{dt} = 0$; therefore

$$[k_1^*] \cdot f \cdot \tau \cdot C_P^* = [k_2^*] \cdot C_{TE}^* \tag{B:9}$$

$$C_{TE}^* = \frac{[k_1^*] \cdot f \cdot \tau \cdot C_P^*}{[k_2^*]}. \tag{B:10}$$

Calculation of $[k_2]$ (7–9)

Since, from Eq. (B:8)

$$\frac{dC_T^*}{dt} = [k_1^*] \cdot f \cdot \tau \cdot C_P^* - [k_2^*] \cdot C_T^* \tag{B:11}$$

$$\frac{dC_T^*}{dt} = [k_2^*] \left(\frac{[k_1^*] \cdot f \cdot \tau \cdot C_P^*}{[k_2^*]} - C_T \right) \tag{B:12}$$

$$\frac{dC_T^*}{dt} = [k_2^*] \cdot (C_{TE}^* - C_T^*) \quad \text{[see Eq. (B:10)]} \tag{B:13}$$

$$[k_2^*] = \frac{\frac{dC_T^*}{dt}}{(C_{TE}^* - C_T^*)}. \tag{B:14}$$

(For description of curve-fitting technique see Eqs. (24) and (25) in text). Since

$$[k_2] = \zeta \cdot [k_2^*] \quad (\zeta = 1.11), \tag{B:15}$$

therefore

$$[k_2] = \zeta \cdot \frac{\frac{dC_T^*}{dt}}{(C_{TE}^* - C_T^*)}. \tag{B:16}$$

Calculation of v_I (7–9)

Since

$$v_I = [k_1^*] \cdot \zeta \cdot f \cdot \tau \cdot C_P \quad (\zeta = 1.11) \tag{B:17}$$

and

$$[k_1^*] \cdot f \cdot \tau = [k_2^*] \cdot \frac{C_{TE}^*}{C_P^*} \quad \text{[see Eq. (B:9)]} \tag{B:18}$$

and

$$[k_2] = \zeta \cdot [k_2^*], \tag{B:19}$$

thus

$$v_I = [k_2] \cdot \frac{C_{TE}^*}{C_P^*} \cdot C_P \tag{B:20}$$

or

$$v_I = [k_2] \cdot C_{TE}^* \cdot \frac{\mu mol\ (G)}{cpm\ (CMG)}\ blood. \tag{B:21}$$

Calculation of κ_1 (7–9)

$$\kappa_1 = \frac{v_I}{C_P} \quad \text{[see Eq. (B:20)]} \tag{B:22}$$

$$\kappa_1 = [k_2] \cdot \frac{C_{TE}^*}{C_P^*} \tag{B:23}$$

and also, from Eq. (B:17),

$$\kappa_1 = [k_1^*] \cdot \zeta \cdot f \cdot \tau \tag{B:24}$$

(For description of curve-fitting technique for finding κ_1 see Eqs. (24) and (25) in text.)

Calculation of K_M', V_{MAX} for Hexose Carrier from Blood to Tissue (8,9)

Since

$$v_I = \frac{V_{MAX} \cdot S}{K_M' + S} \tag{B:25}$$

and from Eq. (B:3)

$$v_I = [k_1] \cdot S \tag{B:26}$$

and from Eq. (B:17)

$$v_I = [k_1] \cdot f \cdot \tau \cdot C_P, \tag{B:27}$$

thus

$$S = f \cdot \tau \cdot C_P. \tag{B:28}$$

Since

$$f \cdot \tau = \frac{[k_2^*]}{[k_1^*]} \cdot \frac{C_{TE}^*}{C_P^*} = A \text{ (a constant)}, \tag{B:29}$$

A is reasonably constant because even though C_{TE}^* and C_P^* change with time, their ratio remains constant. The ratio $[k_2^*]/[k_1^*]$ in 5 here is not known; assuming it to be unity; K_M is designated K_M'. Therefore

$$S = A \cdot C_P \tag{B:30}$$

and from Eqs. (B:3) and (B:26)

$$v_I = [k_1] \cdot S. \tag{B:31}$$

From Eq. (B:25),

$$v_I = \frac{V_{MAX} \cdot S}{K_M' + S}. \tag{B:32}$$

Inverting this equation gives a linear relationship between $\frac{1}{v_I}$ and $\frac{1}{S}$:

$$\frac{1}{v_I} = \frac{1}{V_{MAX}} + \frac{1}{S} \cdot \frac{K_M'}{V_{MAX}}. \tag{B:33}$$

Measurements are made at not less than two different levels of C_P; a plot of $\frac{1}{v_I}$ vs. $\frac{1}{S}$ gives a straight line with intercept $\frac{1}{V_{MAX}}$ and slope $\frac{K_M'}{V_{MAX}}$. Thus, here K_M' has units $\frac{\mu mol}{g}$ and V_{MAX} units of $\frac{\mu mol}{min \cdot g}$.

APPENDIX C

Derivation of C_{TE}, $V_{E,M}$, and $k_{E,M}$

For meaning of symbols see Appendices A and B, Fig. 1, and text.

Calculation for C_{TE} via rate constants

Since

$$v_I = v_E + v_{E,M} \tag{C:1}$$

$$[k_2] \cdot C_P \cdot \frac{C_{TE}^*}{C_P^*} = [k_2] \cdot C_{TE} + k_{E,M} \cdot C_{TE}. \tag{C:2}$$

[see Eq. (B:20)]; thus

$$C_P \cdot \frac{C_{TE}^*}{C_P^*} = C_{TE} \cdot \left(1 + \frac{k_{E,M}}{[k_2]}\right) \tag{C:3}$$

and

$$C_{TE} = C_P \cdot \frac{C_{TE}^*}{C_P^*} \cdot \frac{1}{1 + \frac{k_{E,M}}{[k_2]}} \tag{C:4}$$

or

$$C_{TE} = C_P \cdot \frac{C_{TE}^*}{C_P^*} \cdot F \quad \text{with } F = \frac{1}{1 + \frac{k_{E,M}}{[k_2]}}. \tag{C:5}$$

Calculation of C_{TE} via K_M' and V_{MAX}

From Michaelis-Menten kinetics

$$v_E = \frac{V_{MAX} \cdot C_{TE}}{K_M' + C_{TE}} \tag{C:6}$$

and since $v_E = [k_2] \cdot C_{TE}$,

$$[k_2] = \frac{V_{MAX}}{K_M' + C_{TE}} \tag{C:7}$$

thus

$$C_{TE} = \frac{V_{MAX}}{[k_2]} - K_M'. \tag{C:8}$$

Calculation of $v_{E,M}$

Since

$$v_{E,M} = v_I - v_E \tag{C:9}$$

$$v_{E,M} = v_I - [k_2] \cdot C_{TE} \tag{C:10}$$

thus [see Eqs. (B:20) and (C:5)]

$$v_{E,M} = [k_2] \cdot C_P \cdot \frac{C_{TE}^*}{C_P^*} - [k_2] \cdot C_P \cdot \frac{C_{TE}^*}{C_P^*} \cdot F \tag{C:11}$$

or

$$v_{E,M} = [k_2] \cdot C_P \cdot \frac{C_{TE}^*}{C_P^*} \cdot (1 - F). \tag{C:12}$$

Calculation of $k_{E,M}$

$$k_{E,M} = \frac{v_{E,M}}{C_{TE}}. \tag{C:13}$$

REFERENCES

1. Sokoloff L, Reivich M, Kennedy C, et al: The [C-14] deoxyglucose method for the measurement of local cerebral glucose utilization: Theory, procedure, and normal values in the conscious and anesthetized albino rat. *J Neurochem* 28:897–916, 1977
2. Reivich M, Kuhl D, Wolf A, et al: The [F-18] fluorodeoxyglucose method for the measurement of local cerebral glucose utilization in man. *Circ Res* 44:127–137, 1979
3. Phelps ME, Huang SC, Hoffman EJ, et al: Tomographic measurement of local cerebral glucose metabolic rate in humans with [F-18]-2-fluorodeoxy-D-glucose: Validation of method. *Ann Neurol* 6:371–388, 1979
4. Betz AL, Gilboe DD, Yudilevich DL, et al: Kinetics of unidirectional glucose transport into the isolated drug brain. *Am J Physiol* 225:586–592, 1973
5. Pardridge WM, Oldendorf WH: Kinetics of blood-brain barrier transport of hexoses. *Biochim Biophys Acta* 382:377–392, 1975
6. Kloster G, Müller-Platz C, Laufer P: 3-11-C-methyl-D-glucose: A potential agent for regional cerebral glucose utilization. Synthesis, chromatography, and tissue distribution in mice. *J Lab Comp Radiopharm* 18:855–863, 1981
7. Vyska K, Freundlieb C, Höck A, et al: Analysis of local perfusion rate (LPR) and local glucose transport rate (LGTR) in brain and heart in man by means of C-11-methyl-D-glucose (CMG) and dynamic positron emission tomography (dPET). In *Radioaktive Isotope in Klinik und Forschung*, Vol. 15, Höfer R, Bergmann H, Eds. Vienna, Verlag H. Egermann, 1982, pp 129–142
8. Vyska K, Profant M, Schuier F, et al: In vivo determination of kinetic parameters for glucose influx and efflux by means of 3-O-^{11}C-methyl-D-glucose, ^{18}F-3-deoxy-3-fluoro-D-glucose and dynamic positron emission tomography: Theory, method and normal values. In *Current Topics in Tumor Cell Physiology and Pos-*

itron Emission Tomography, Knapp WH, Vyska K, Eds. Berlin, Springer-Verlag, 1984, pp 37–60
9. Vyska K, Magloire JR, Freundlieb C, et al: In vivo determination of the kinetic parameters of glucose transport in the human brain using ^{11}C-methyl-D-glucose (CMG) and dynamic positron emission tomography (dPET). *Eur J Nucl Med* 11:97–106, 1985
10. Gjedde A, Diemer NH: Autoradiographic determination of regional brain glucose content. *J Cereb Blood Flow Metab* 3:303–310, 1983
11. Oldendorf WH: Brain uptake of radiolabelled amino acids, amines, and hexoses. *Am J Physiol* 221:1629–1639, 1971
12. Lund-Andersen H: Transport of glucose from blood to brain. *Physiol Rev* 59:305–352, 1979
13. Gjedde A: Calculation of cerebral glucose phosphorylation from brain uptake of glucose analogs in vivo: A re-examination. *Brain Res* 4:237–274, 1982
14. Gjedde A: Modulation of substrate transport to the brain. *Acta Neurol Scand* 67:3–25, 1983
15. Crone C: Om diffusionen af nogle organiske nonelektrolyte fra blod til kjerne vaer. Thesis, University of Copenhagen, Copenhagen, Munksgaard Publishing, 1961
16. Narahara HT, Özand P, Cori CF: Studies of tissue permeability. VII. The effect of insulin on glucose generation and phosphorylation in frog muscle. *J Biochem* 235:3370–3378, 1960
17. Lassen NA, Gjedde A: Kinetic analysis of the uptake of glucose and some of its analogs in the brain using the single capillary model: Comments on some points of controversy. In *Lecture Notes in Biomathematics 48, Tracer Kinetics and Physiological Modeling*, Lambrecht RM, Rescigno A, Eds. Berlin, Springer-Verlag, 1983, pp 387–410
18. Sokoloff L, Smith CB: Basic principles underlying radioisotopic methods for assay of biochemical processes in vivo. In *Lecture Notes in Biomathematics 48, Tracer Kinetics and Physiological Modeling*, Lambrecht RM, Rescigno A, Eds. Berlin, Springer-Verlag, 1983, pp 201–233
19. Gjedde A, Wienhard K, Heiss W-D, et al: Comparative regional analysis of 2-fluorodeoxyglucose and methylglucose uptaken in brain of four stroke patients, with special reference to the regional estimation of the lumped constant. *J Cereb Blood Flow Metab* 5:163–178, 1985
20. Budinger TF, Huesmann RH, Knittel B, et al: Physiological modelling of dynamic measurements of metabolism using positron emission tomography. In *The Metabolism of the Human Brain Studied with Positron Emission Tomography*, Greitz T et al, Eds. New York, Raven Press, 1985, pp 165–183
21. Lammertsma AA, Wise RJS, Jones T, et al: Correction for the presence of intravascular oxygen-15 in the steady-state technique for measuring regional oxygen extraction ratio in the brain, 2. Results in normal subjects and brain tumor and stroke patients. *J Cereb Blood Flow Metab* 3:425–431, 1983
22. Frackowiak RSJ, Lenzi G-L, Jones T, et al: Quantitative measurement of regional cerebral blood flow and oxygen metabolism in man using ^{15}O and positron emission tomography. *J Comput Assist Tomogr* 4:727–736, 1980
23. Feinendegen LE: The dual parameter analysis for in vivo measurement of metabolic reactions. In *Radioaktive Isotope in Klinik und Forschung*, Vol. 16, Höfer R, Bergmann H, Eds. Vienna, Verlag H. Egermann, 1984, pp 465–486
24. Huang M-T, Veech RL: Metabolic fluxes between ^{14}C-2-deoxy-D-glucose and ^{14}C-2-deoxy-D-glucose-6-phosphate in brain in vivo. J. Neurochem 44:567–573, 1985
25. Roland PE, Larsen B: Focal increase of cerebral blood flow during stereognostic testing in man. *Arch Neurol* 33:551–558, 1976
26. Vyska K, Freundlieb C, Höck A, et al: Simultaneous measurement of local perfusion rate (LPR) and glucose transport rate (LGTR) in brain and heart, with C-11-methylglucose (CMG) and dynamic positron emission tomography (dPET). *J Nucl Med* 23:P13, 1982 (abstr)
27. Schelbert HR: The heart. In *Computed Emission Tomography*, Ell PJ, Holman BJ, Eds. Oxford, Oxford University Press, 1982, pp 91–133
28. Halama JR, Holden JE, Gatley SJ, et al: Studies of glucose transport using F-18 fluorosugars. *J Nucl Med* 23:79, 1982
29. Halama JR, Holden JE, Gatley SJ, et al: Validation of F-18-deoxy-3-fluoro-D-glucose (3-FDG) as an agent for measurement of glucose transport by positron emission tomography. *J Nucl Med* 24:P72, 1983 (abstr)